J Mater Sci (2008) 43:23–32
DOI 10.1007/s10853-007-1985-z

Brazing of yttria-stabilized zirconia (YSZ) to stainless steel using Cu, Ag, and Ti-based brazes

Mrityunjay Singh · Tarah P. Shpargel · Rajiv Asthana

Received: 30 April 2007 / Accepted: 9 July 2007 / Published online: 8 November 2007

Abstract Copper and silver-base active metal brazes containing Ti (Cu-ABA, Ticusil, and Ticuni) were tested for oxidation resistance to 750–850 °C, and for their effectiveness in joining yttria-stabilized-zirconia (YSZ) to a corrosion-resistant ferritic stainless steel. The braze oxidation behavior was characterized using thermogravimetric analysis (TGA), optical and scanning electron microscopy (SEM), and energy dispersive spectrometry (EDS). Ticusil and Ticuni at 750 °C exhibited sluggish oxidation kinetics whereas Copper-ABA at 850 °C displayed the fastest kinetics and relatively large weight gain. The SEM and EDS examination of the steel/braze and YSZ/braze interfaces showed the dissolution of Y and Zr from YSZ in braze, diffusion of Ag in the YSZ, and formation of a thin Ti-rich interphase between YSZ and Ti-base brazes. These compositional changes and interface reconstruction yielded metallurgically sound joints. The Knoop microhardness profiles showed a rather abrupt discontinuity across the YSZ/braze interfaces and a more uniform distribution across the steel/braze interface.

M. Singh (✉)
Ohio Aerospace Institute, NASA Glenn Research Center, Cleveland, OH 44135, USA
e-mail: msingh@grc.nasa.gov

T. P. Shpargel
ASRC Aerospace Corp., NASA Glenn Research Center, Cleveland, OH 44135, USA

R. Asthana
Engineering and Technology Department, University of Wisconsin-Stout, Menomonie, WI 54751, USA

Introduction

Solid oxide fuel cells (SOFC) are a promising technology and their commercial exploitation requires development of manufacturing techniques that are capable of assembling and joining oxides and metals. Among the current ceramic joining techniques, active metal brazing is a simple and cost–effective method, and has attracted considerable attention for creating oxide/metal joints for use in SOFCs [1, 2]. Some considerations in selecting the braze alloy composition for SOFC applications include: (1) wettability of molten braze on oxide substrate, (2) adhesion upon solidification, (3) resistance to oxidation, corrosion, grain coarsening and creep at the SOFC operating temperatures (700–900 °C), and (4) thermal stress induced by temperature excursions and difference in the coefficients of thermal expansion (CTE) of braze filler and oxide substrate. The fundamental requirements of good wetting and flow have led to the development of active metal brazes containing reactive solutes such as Ti, V, or Cr, that enhance the metal–ceramic wettability by inducing chemical reactions at the joint during brazing [3–11].

Copper and silver are widely used as base filler metals because of their chemical inertness, ductility, and good fluidity in molten state. Both are excellent conductors of heat and electricity, factors critical for SOFC joints; the high thermal conductivity of Cu (398 W/m K) and Ag (428 W/m K) enables rapid heat dissipation at the joint, and the high electrical conductivity ($6.0 \times 10^7\ \Omega^{-1}\ m^{-1}$ for Cu and $6.8 \times 10^7\ \Omega^{-1}\ m^{-1}$ for Ag) meet the basic electrical conductivity requirements for SOFC applications. The large ductility of Cu and Ag is beneficial to the accommodation of thermal stresses that develop during joint fabrication and SOFC operation due to the CTE mismatch (CTE of YSZ is 8.9–10.6 $\times\ 10^{-6}$/K, and the CTE of Cu and

Ag are 17.0 × 10^{-6}/K and 19.7 × 10^{-6}/K, respectively). Additionally, the relative chemical inertness of Ag and Cu is beneficial for oxidation resistance at the high operating temperatures of SOFCs.

In this paper, three commercial copper- and silver braze alloys (Copper-ABA, Ticuni and Ticusil), all containing Ti as the active metal, were tested for their oxidation resistance at elevated temperatures, and for their effectiveness in forming microstructurally sound joints between yttria-stabilized zirconia and stainless steel. The oxidation behavior of the braze materials in air was examined by thermogravimetric analysis (TGA), and the microstructure and composition of the oxidized braze foils and brazed YSZ/steel joints were examined by optical and scanning electron microscopy (SEM) coupled with energy dispersive spectrometry (EDS). The distribution of hardness across the joints was determined by using a Knoop microindentation test.

Experimental procedures

A corrosion-resistant ferritic stainless steel from Allegheny-Ludlum, and yttria-stabilized zirconia substrates (containing 3 mol% yttria) were used to simulate the SOFC joint interface. The steel substrates (1.01 mm thick) nominally contained 17–19% Cr, and minor alloying elements, such as Mn, P, Si, Ni, and Ti. The YSZ substrates were made by tape casting and sintering. The YSZ substrate thickness after sintering was ~1.63 mm. The braze alloys (Cu-ABA®, Ticuni®, and Ticusil®) were in the form of foils (0.10–0.12 mm thick), and were obtained from Morgan Advanced Ceramics, CA. The nominal compositions and selected physical and mechanical properties of these brazes are listed in Table 1.

The braze oxidation behavior was characterized with a Thermo Gravimetric Analyzer (TGA) in air at 850 °C for Cu-ABA and 750 °C for Ticusil and Ticuni for up to 200 min. Plots of the mass gain-to-surface area ratio versus time as well as mass gain-to-surface area ratio versus the square root of time were developed to evaluate the oxidation kinetics. The surfaces of oxidized foils were examined by SEM and EDS (model JEOL-840) before and after the oxidation tests. The reason for choosing an oxidation temperature of 850 °C for Cu-ABA and 750 °C for Ticusil and Ticuni is that the liquidus temperature of Cu-ABA (T_L = 1,297°K) is higher than the liquidus temperatures of Ticuni (T_L = 1,233°K) and Ticusil (T_L = 1,173°K). The oxidation temperatures were selected to be about 30% above two-third's of the absolute liquidus temperature of the alloy. For Cu-ABA, an oxidation temperature of 850 °C (1,123 K) is 30% above (2/3)T_L, and for Ticusil, an oxidation temperature of 750 °C (1,023°K) is 30% above (2/3)T_L. For Ticuni, the oxidation temperature of 750 °C is 25% above (2/3)T_L, which is still not too far from the 30% target.

The joining procedure consisted of placing a braze foil between the YSZ and steel substrates, each measuring 1.25 cm × 1.25 cm in cross section. A normal load of 0.3 N was applied to each joint. The assembly was heated under vacuum (~10^{-6} torr) to the brazing temperature (typically 10–15 °C above the liquidus). After an isothermal soak of 5 min at the brazing temperature, the joint was furnace cooled at a controlled rate. The samples were cut on a low-speed diamond saw, mounted in epoxy, and polished for microstructural examination using optical microscopy, SEM, and EDS. The EDS data, given in atom percent (at%) are qualitative and represent the relative atomic percentage of the alloying elements at the locations marked in corresponding SEM photomicrographs. Microhardness measurements were made across the joint interfaces using a Knoop micro-indenter on a Buehler's MicroMet-2001 machine under a load of 200 g and a loading time of 10 s.

Results and discussion

Braze oxidation behavior

Figure 1 shows the results of the TGA as normalized percent weight gain per unit surface area of oxidized Ticusil, Ticuni, and Cu-ABA foils as a function of oxidation time. An initial transient oxidative phase was noted for all brazes during which the kinetics fluctuated randomly. Figure 1 shows that Cu-ABA at 850 °C exhibits the fastest oxidation kinetics, followed by Ticusil and Ticuni at 750 °C, with both the latter brazes exhibiting nearly

Table 1 Physical and mechanical properties of braze alloys used in the study

Braze	Composition, wt%	T_L, K	T_S, K	E, GPa	YS, MPa	UTS, MPa	CTE, $\times 10^{-6}$ K^{-1}	Thermal conductivity, W/m K	%Elong.	Electrical conductivity, $\times 10^{6}$ Ω^{-1} m^{-1}
Ticusil	68.8Ag–26.7Cu–4.5Ti	1,173	1,053	85	292	339	18.5	219	28	29
Ticuni	15Cu–15Ni–70Ti	1,233	1,183	144	–	–	20.3	–	–	–
Cu-ABA	92.8Cu–3Si–2Al–2.25Ti	1,297	1,231	96	279	520	19.5	38	42	5.1

Source: http://www.wesgometals.com/framet2.html

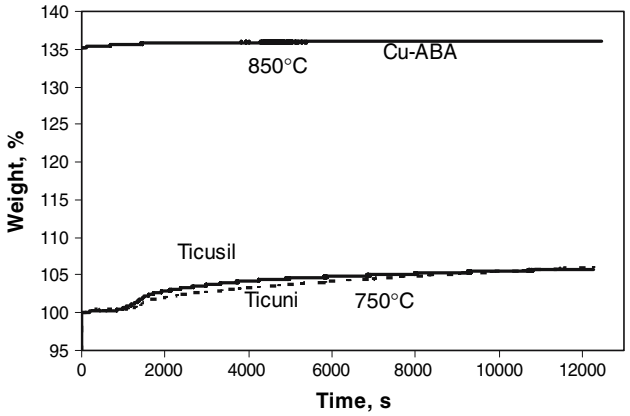

Fig. 1 Oxidation kinetics as percent weight gain per unit surface area for Cu-ABA at 850 °C, and Ticusil and Ticuni braze foils in air at 750 °C

identical kinetics. Whereas Cu-ABA appears to rapidly attain saturation weight Ticusil and Ticuni exhibit a more complex oxidation behavior, and a more gradual approach to a limiting weight gain. The main constituent of Ticusil is silver, whose oxide (Ag_2O) has a Pilling-Bedworth (PB) ratio of 1.59, between 1 and 2, and will, therefore, be expected to form a protective oxide scale. The PB ratios of oxides of Cu are 1.68 (Cu_2O) and 1.74 (CuO), which are slightly higher than that of Ag_2O. Interestingly, however, whereas Cu forms a protective scale, silver is known to form an unstable and non-protective Ag_2O scale [12] even though its PB ratio is between 1 and 2. While 26.7% Cu in the silver braze, Ticusil, will impart some protection against oxidation, its large Ag content (68.8%) will likely dominate the oxidation response. The formation of an unstable Ag_2O scale is the probable reason for the relatively rapid oxidation kinetics of Ticusil than Ticuni at the lower temperature of 750 °C.

The PB ratio of Ni is 1.52, which suggests that Ni forms a protective oxide scale. The PB ratios of the various titanium oxides also indicate the formation of relatively protective scales. For example, the PB ratios of TiO_2 (density: 4 g cm^{-3}), TiO (4.08 g cm^{-3}), Ti_2O_3 (4.9 g cm^{-3}), and Ti_3O_5 (4.6 g cm^{-3}) are 1.95, 1.47, 1.38, and 1.53, respectively, all of which are less than 2. Generally, a PB ratio greater than 2 indicates an unstable scale, likely to continuously flake off because the oxide volume is significantly greater than the volume of metal consumed in the oxidation reactions. In the case of Cu-ABA (92.8Cu–3Si–2Al–2.5Ti), the very large Cu content (92.8%) will protect it against further oxidation (Cu_2O and CuO have PB < 2); however, the higher oxidation temperature of 850 °C used for Cu-ABA has lead to relatively large weight gain ($\sim$135%). The alloying elements Si and Al in Cu-ABA also form protective scales; the PB ratios of Si and Al are 2.27 and 1.28, respectively (Si exhibits an anomalous behavior in that even though its PB ratio >2, it is known to form a protective scale).

The Gibb's free energies of oxide formation of the various braze constituents (Ag, Cu, Ti, Ni, Al, and Si) were calculated as a function of temperature using the software HSC Chemistry version 4.1 (Outokumpu Ra, Oy, Finland). The following standard oxides were considered: Ag_2O, NiO, CuO, Cu_2O, SiO_2, Al_2O_3, TiO, TiO_2, Ti_2O_3, Ti_3O_5, and Ti_4O_7. The calculated ΔG values of oxides are plotted in Fig. 2 as a function of temperature. These calculations suggest that the primary oxides of Ti have the largest negative ΔG values from room temperature to the oxidation temperatures of 750–850 °C, and are, therefore, thermodynamically most stable among the oxides considered above. The oxides of Al and Si also have relatively large negative ΔG values, but are somewhat less than oxides of Ti. The oxides of copper (CuO and Cu_2O) and nickel (NiO) also have negative ΔG values at the oxidation temperature, but will be appreciably less stable than the oxides of Ti, Al, and Si. In contrast, the oxide of silver is unstable at all temperatures as indicated by its positive free energy change. Titanium is a constituent of all the three brazes, and possesses a strong affinity for oxygen. The

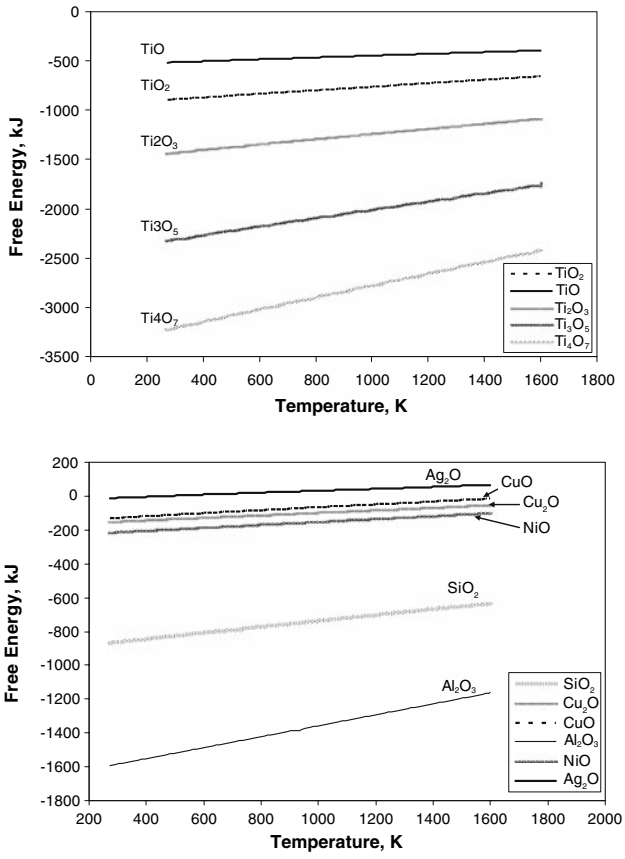

Fig. 2 Free energy of oxide formation for common oxides of (**a**) titanium and (**b**) elements Si, Al, Cu, Ni, and Ag as a function of oxidation temperature

Gibb's free energy of oxide formation, ΔG, for the oxides of Ti at the oxidation test temperature of 750 °C (Ticuni and Ticusil) are (in kJ): TiO_2 (−758.4), TiO (−444.1), Ti_4O_7 (−2764.4), and Ti_3O_5 (−2000.9). Similarly, the ΔG values for these oxides at 850 °C (Cu-ABA) are (in kJ): TiO_2 (−740.7), TiO (−434.9), Ti_4O_7 (−2704.9), and Ti_3O_5 (−1959.1). These negative free energy values show that formation of titanium oxides is highly probable at both test temperatures.

In order to determine the chemical redistribution of elements during oxidation, SEM examination and EDS map scans were done on as-received foils and post-TGA foils. These scans for the three brazes are shown in Figs. 3–5. From the SEM images of oxidized and as-received braze foils, it is clear that chemical and structural changes have occurred on the surface of the braze foils. The oxidized braze foils show the presence of oxygen at the surface. Thus, EDS mapscans of oxidized brazes suggest possible formation of oxides of Cu, Al and Ti. A change in the surface morphology after oxidation is also evident.

The oxidation data on braze foils actually represent a 'worst case' scenario where the surface areas exposed to the oxidizing atmosphere are much larger than the exposed braze surface area in an actual joint. There is, however, a distinct possibility that the braze alloy–substrate interactions shall modify the structure and metallurgy of the joint, which in turn, might alter the joint's oxidation response. While the actual oxidation kinetics of brazed joints were not evaluated in the present work, there is some evidence in the literature [13] to suggest that significant changes in either the bond strength or the microstructure may not occur in as-bonded and oxidized joints made using active braze alloys.

Microstructure and Chemistry of the Joint

YSZ/Ticuni/Steel Joint

Figure 6 shows the microstructure of the YSZ/Ticuni/steel joint after brazing at 975 °C for 5 min in vacuum.

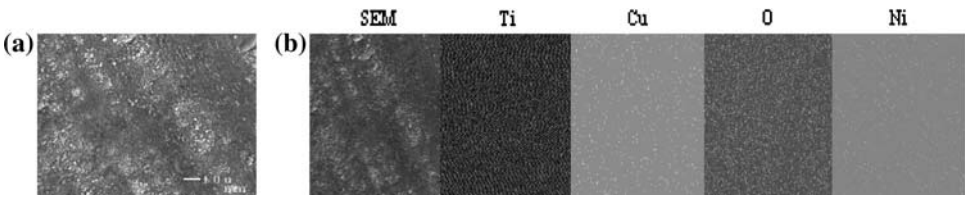

Fig. 3 (**a**) Microstructure and (**b**) X-ray dot map of Ticuni foil, oxidized in air at 750 °C

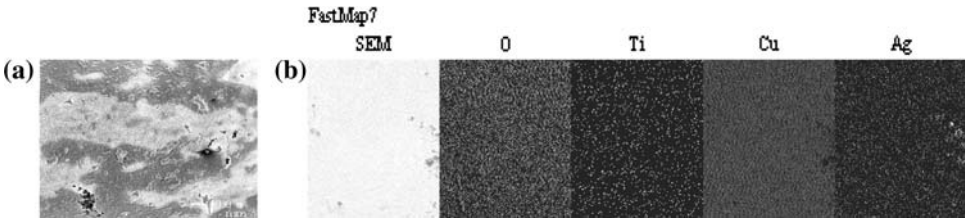

Fig. 4 (**a**) Microstructure and (**b**) X-ray dot map of Ticusil foil, oxidized in air at 750 °C

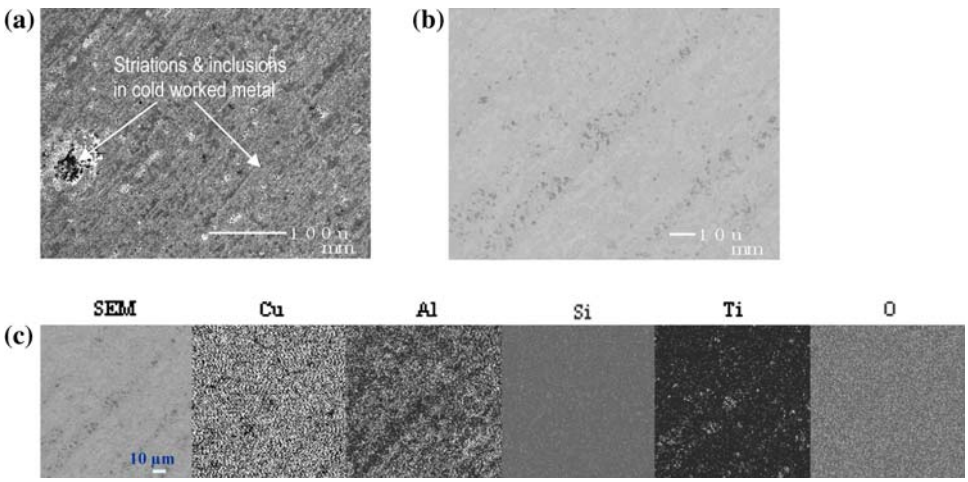

Fig. 5 (**a**) Secondary electron image, (**b**) backscattered image, and (**c**) X-ray dot map of Cu-ABA foil, oxidized in air at 850 °C

The optical (Fig. 6a, b) and SEM (Fig. 6c, d) views of the joints suggest formation of metallurgically sound joints. However, there is evidence of dispersed voids, visible at high magnification (Fig. 6c), in the braze region adjacent to the braze/steel interface. Such voids could either represent micro-shrinkage which is characteristic of long-freezing range alloys that exhibit protracted semi-solid region. Whereas the freezing range of virgin Ticuni (Table 1) is only 50° K, the extensive dissolution of steel constituents in molten braze could alter the freezing range, and lead to dispersed voids as noted in Fig. 6c. A closer examination of the voids in Fig. 6c indicates these to be roughly spherical in shape, which is more typical of entrapped or evolving gaseous products rather than solidification shrinkage. The dissolution of steel in molten Ticuni braze has occurred in the contact region, and the braze/steel interface is diffused (Fig. 6c). The EDS composition analysis (Table 2) indicates that Ti from braze has diffused into the steel, and Cr and Fe from the steel have diffused into braze thus establishing composition gradients across the diffused interface. At the Ticuni/YSZ interface (Fig. 6d) a reaction layer has formed; evidence of micro-cracks within this reaction layer is noted. The EDS results show that the reaction layer contains Zr, Ti, and Y (point 2, Fig. 6d). There is some dissolution of YSZ in braze as indicated by the presence of Zr and Y within the braze (point 1, Fig. 6d), and there is evidence of Ti diffusion into the YSZ-side of the reaction layer (point 3, Fig. 6d). Far from the interface into the YSZ (point 4, Fig. 6d), the original composition is restored.

YSZ/Ticusil/steel joint

The microstructure of the YSZ/Ticusil/steel joint after brazing at 910 °C for 5 min in vacuum is shown in Fig. 7. A microstructurally sound joint devoid of interfacial voids and microcracks has formed. The steel/Ticusil interface is more diffused than the YSZ/Ticusil interface (Fig. 7c), due to greater dissolution and interdiffusion at the metal/metal interface. The relative percentages among the alloying elements are shown in Table 3. Titanium has diffused into the steel substrate (point 1, Fig. 7d), and Cr and Fe from steel have diffused into the braze (point 4, Fig. 7d). The interface is enriched in titanium; the highest Ti concentration occurs within the interface region (point 3). At the YSZ/Ticusil interface (Fig. 7e), Zr and Y have dissolved in the braze (point 1), and Ag has diffused into the YSZ (point 4). A dark, titanium-rich reaction layer has formed between the YSZ and Ticusil; this layer also contains Zr and Ag (point 3, Fig. 7e). Titanium-enrichment at the YSZ surface depletes the YSZ of oxygen, thus creating a dark, O-deficient YSZ region as also reported by other investigators [7].

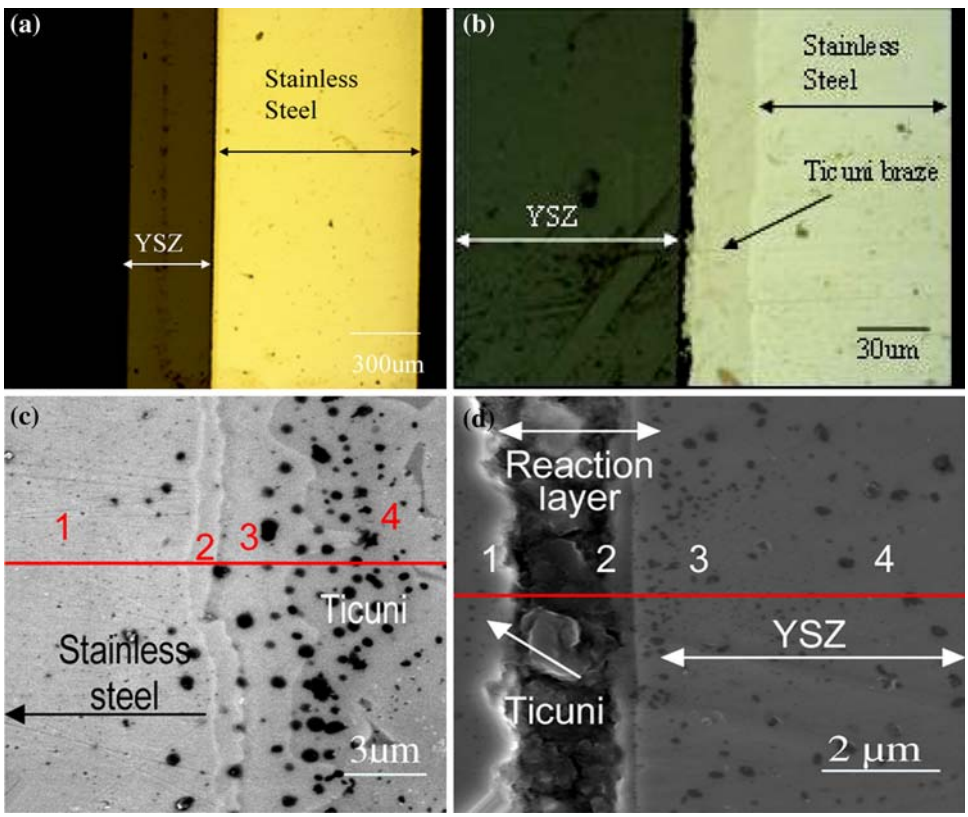

Fig. 6 Microstructure of YSZ/Ticuni/Steel joint: (**a**) & (**b**) are optical views, and (**c**) & (**d**) SEM views showing diffusion zone and reaction layer formation at the joint. (**c**) & (**d**) also show EDS composition analyses at marked points at (**c**) steel/Ticuni interface, and (**d**) YSZ/Ticuni interface. The compositions are given in Table 2

Table 2 EDS composition analysis (at%) for YSZ/Ticuni/stainless steel joint (Fig. 6)

	Fe	Cr	Ni	Y	Zr	Cu	Ti
Point 1, Fig 6(c)	78	20	–	–	–	–	2
Point 2, Fig 6(c)	61	14	–	–	–	–	25
Point 3, Fig 6(c)	17	8	23	–	–	21	32
Point 4, Fig 6(c)	10	6	15	–	–	24	44
Point 1, Fig 6(d)	11	–	23	1	3	6	56
Point 2, Fig 6(d)	–	–	–	22	47	–	31
Point 3, Fig 6(d)	–	–	–	–	29	–	71
Point 4, Fig 6(d)	–	–	–	7	93	–	–

The data show relative atomic percentages of the alloying elements

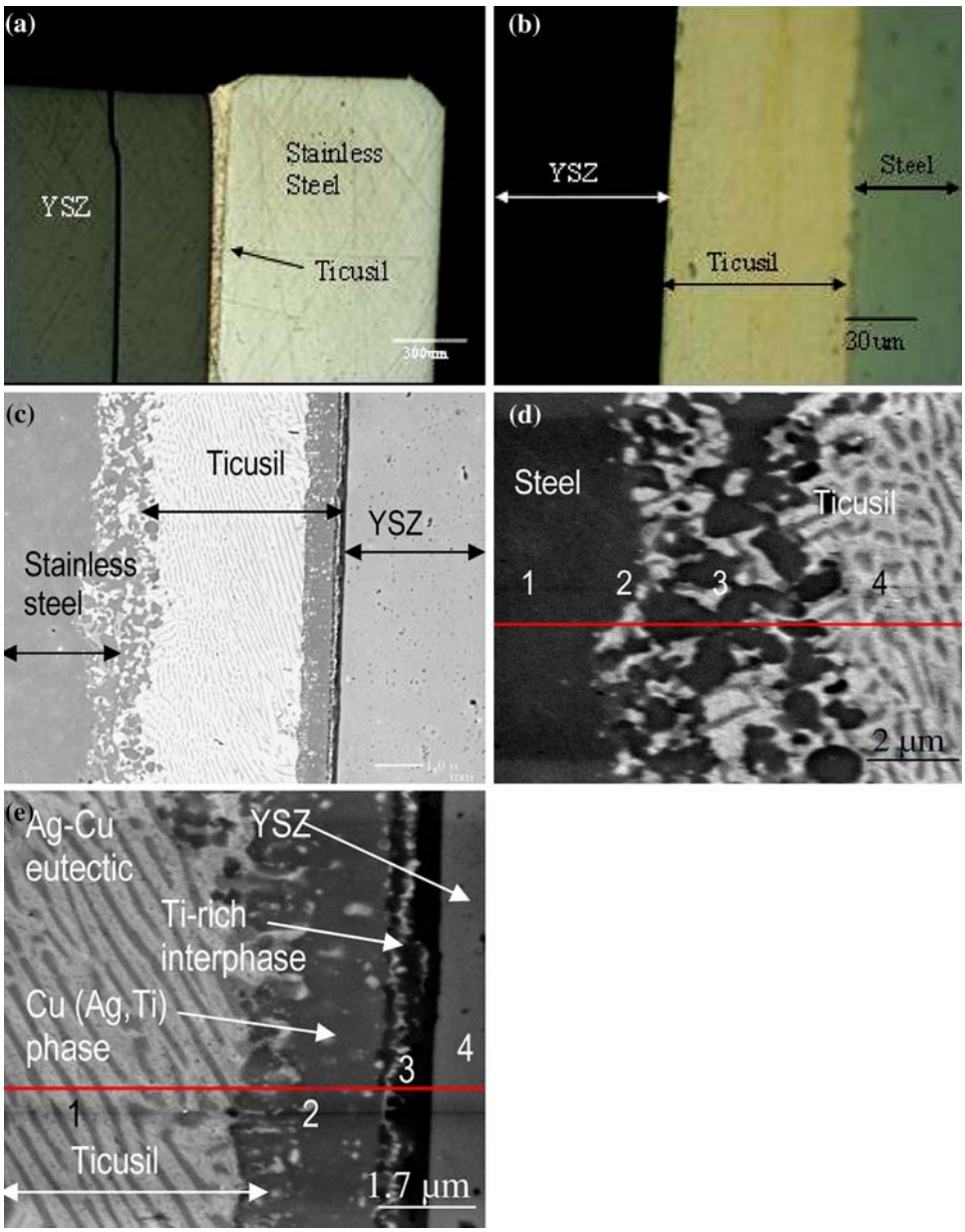

Fig. 7 Microstructure of the YSZ/Ticusil/Steel joint: (**a**) & (**b**) optical views, and (**c**) SEM view. (**d**) & (**e**) show EDS composition analysis at (**d**) steel/Ticusil interface and (**e**) Ticusil/YSZ interface, respectively. The compositions at marked points in (**d**) & (**e**) are given in Table 3

Adjacent to this well-defined reaction layer is a somewhat diffused layer containing the elements Ti, Cu, Ag, Zr, and Y. Within the braze region (point 4 in Fig. 7d and point 1 in Fig. 7e), a lamellar Ag–Cu eutectic phase mixture has formed in which the constituent phases also contain Fe, Cr, and Ti (in the eutectic at the steel/braze interface, Fig. 7d),

Table 3 EDS composition analysis (at%) for YSZ/Ticusil/stainless steel joint (Fig. 7)

	Ag	Fe	Cr	Y	Zr	Cu	Ti
Point 1, Fig 7(d)	7	61	27	–	–	–	5
Point 2, Fig 7(d)	30	10	7	–	–	45	8
Point 3, Fig 7(d)	12	51	16	–	–	–	21
Point 4, Fig 7(d)	51	10	9	–	–	22	8
Point 1, Fig 7(e)	60	–	–	3	3	28	6
Point 2, Fig 7(e)	13	–	–	4	8	23	52
Point 3, Fig 7(e)	8	–	–	–	14	–	78
Point 4, Fig 7(e)	17	–	–	3	80	–	–

The data show relative atomic percentages of the alloying elements

and Ti, Zr, and Y (in the eutectic at the YSZ/braze interface, Fig. 7e), possibly in a solid solution form. In Ticusil, Cu–Ti intermetallic compounds could form upon solidification, such as AgTi, Ti_2Cu_3, and $TiCu_2$.

The Ti content (4.5%) of Ticusil is high enough to ensure activity for chemical reactions and good wettability; however, the Ti contents are not so high as to destroy the ductility of the Ag–28Cu eutectic, or its fluidity in the molten state. The Ag–Cu–Ti system contains a liquid miscibility gap, and the eutectic Ag–Cu alloys containing 5 at% Ti partition the alloy into a Ti-depleted liquid and a Ti-rich liquid [4]. This Ti-rich liquid reacts with the ceramic to form a metallurgical bond [4]. The Ti-depleted liquid forms Ag[Cu,Ti] solid solution upon solidification, and eutectic type phase mixtures as seen in Fig. 7d and e. The Ti-rich liquid solidifies to yield TiCu intermetallics and Ag[Cu] precipitates.

YSZ/Cu-ABA/steel joint

In the YSZ/Cu-ABA/steel joints (Fig. 8) formed at 1040 ^oC in vacuum, considerable chemical diffusion at the steel/Cu-ABA interface (Fig. 8c) has modified the joint composition as well as the interface morphology. The EDS elemental distributions are shown in Table 4. Some Fe and Cr have diffused from the steel into the braze region, and some Al, Si, and Ti from braze have diffused across the interface into the steel (Fig. 8c). The interface morphology is rather rough, but somewhat better demarcated than the steel/Ticuni interface of Fig. 6c. At the YSZ/Cu-ABA interface (Fig. 8d), a Ti- and Zr-rich interface reaction layer has formed; this layer also contains Al and Si (from the braze), and Y (from the YSZ). There is, however, no evidence of the Cu-ABA constituents within the YSZ far from the interface (point 3, Fig. 8d).

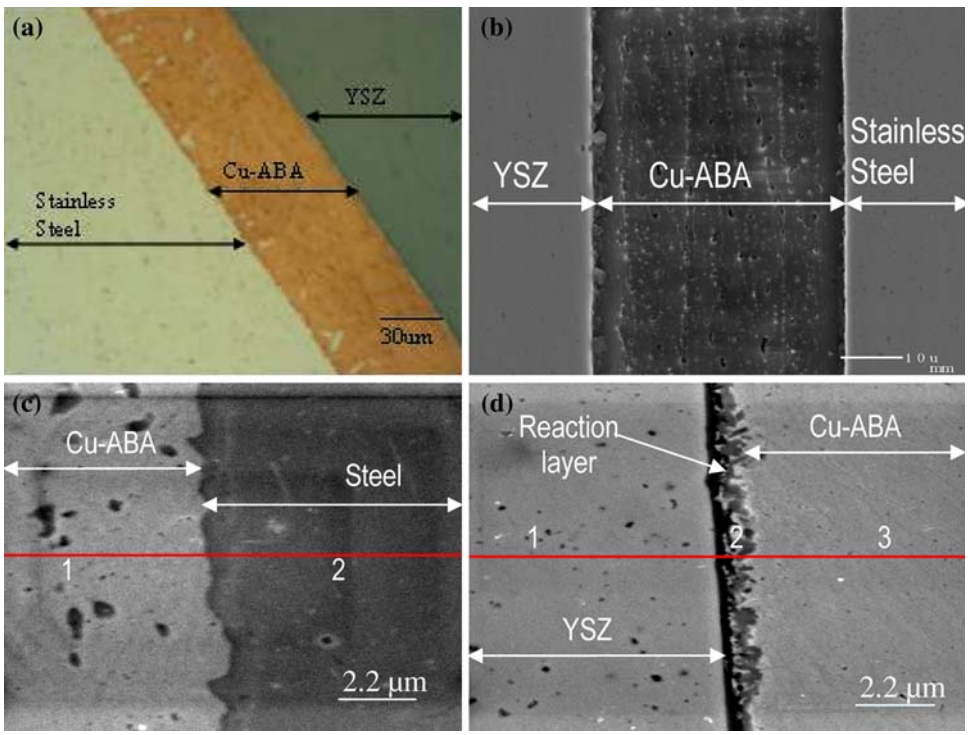

Fig. 8 Microstructure of stainless steel/Cu-ABA/YSZ joint: (**a**) optical view, and (**b–d**) SEM views. (**c**) & (**d**) Show EDS composition analyses at (**c**) Cu-ABA/steel interface, and (**d**) YSZ/Cu-ABA interface. The compositions at marked points in (**c**) & (**d**) are given in Table 4

Table 4 EDS composition analysis (at%) for YSZ/Cu-ABA/stainless steel joint (Fig. 8)

The data show relative atomic percentages of the alloying elements

	Fe	Cr	Y	Zr	Cu	Ti	Si	Al
Point 1, Fig 8(c)	3	2	–	–	80	6	5	3
Point 2, Fig 8(c)	64	19	–	–	–	1	8	8
Point 1, Fig 8(d)	–	–	14	85	–	–	–	–
Point 2, Fig 8(d)	–	–	12	29	–	29	14	16
Point 3, Fig 8(d)	–	–	12	13	60	4	3	8

Reactions, wetting, and braze flow

The possibility of chemical reactions between the braze constituents and the YSZ is considered next. Some possible chemical reactions between the zirconia and yttria of the YSZ and the alloying elements Ti, Al, Si, and Ni in the brazes used in the study are listed in Table 5. The corresponding chemical free energy changes are plotted in Fig. 9 as a function of temperature. The calculations were made using the software HSC Chemistry version 4.1 (Outokumpu Ra, Oy, Finland). The large positive ΔG values for these reactions rule out the formation of oxides by the direct reduction of zirconia and yttria of the YSZ by the braze constituents such as Ti. It might, however, be possible for these oxides to form from the reaction of Ti with the residual oxygen in the brazing furnace atmosphere, if not from the direct chemical reduction of ZrO_2 and Y_2O_3 of YSZ. It has been proposed [7] that Ti can partially deplete the zirconia of oxygen (probably through Ti–O complex formation), and the freed-up oxygen atoms form titanium oxide because the ΔG values for the Ti oxide formation at the brazing temperature are negative. For example, the Gibb's free energy, ΔG, for oxide formation in the brazing temperature range of 1,193–1,253 K for the various oxides of Ti (in kJ) are: TiO_2 (−706.9 to −724.7), TiO (−417.5 to −428.5), Ti_4O_7 (−2590.7 to −2662.9), and Ti_3O_5 (−1878.9 to −1929.7). These negative free energy values show that formation of titanium oxides is probable.

Finally, we consider braze wetting and flow behaviors. The spreading of braze on steel can be characterized by the wetting index [14] (WI), where WI = (Area covered by the braze metal) × cos θ. Higher the value of WI, the better is the wetting and spreading; WI > 0.05 indicates good spreading, and WI > 0.10 indicates excellent spreading. Whereas WI of Ticuni, Ticusil and Cu-ABA on steel could not be found, the WI values of Ag–Cu–Ni brazes on stainless steels (316 and 304 grades) are given in Table 6 at different joining temperatures. The data show that the wetting of Ag–Cu–Ni brazes on steels is generally good. The braze WI data on YSZ are not available, but wetting can be understood in terms of the surface tension, σ_{lv}, contact angle, θ, and work of adhesion ($W_{ad} = \sigma_{lv}(1 + \cos\theta)$). The relatively large σ_{lv} values of the braze constituents suggests that they will not wet the YSZ; for example, σ_{lv} for Ni is 1,796 mN/m (1,455 °C), for Ag it is 925 mN/m (960 °C), and for Cu it is 1,330 mN/m (1,085 °C), respectively [15]. The temperature-corrected surface tension data [15] also do not show any significant drop in σ_{lv} at higher temperatures. The literature data on θ, and W_{ad} of various braze- and steel constituents in contact with the YSZ are listed in Table 7. The addition of Ti improves the wetting (provided Ti in braze is not oxidized by residual oxygen in the furnace). These improvements result from the chemical interactions which include YSZ dissolution in the braze and compound layer formation [21, 22].

The wetting of Ti-containing brazes on oxide ceramics is excellent but relatively slow; for example, Ag–38Cu–3.7Ti droplets spread at a rate of $\sim 6 \times 10^{-4}$ mm s^{-1} on Al_2O_3 substrates at 950 °C [5]. The radius, $R(t)$, of the contact circle between the oxide and the molten braze, was found to increase exponentially with time ($R(t) = R_0 \exp(t/3\tau)$, where R_0 is the initial contact radius and τ is a constant, ~10 min). In our experiments, the joints were

Table 5 Possible chemical reactions of braze constituents (Ti, Al, Si, Ni) and YSZ

Possible reactions with ZrO_2	Possible reactions with Y_2O_3
$ZrO_2 + Ti \rightarrow Zr + TiO_2$	$Y_2O_3 + 2Ti \rightarrow Ti_2O_3 + 2Y$
$ZrO_2 + 2Ti \rightarrow Zr + 2TiO$	$Y_2O_3 + (9/5)Ti \rightarrow (3/5)Ti_3O_5 + 2Y$
$ZrO_2 + (4/3)Ti \rightarrow Zr + (2/3)Ti_2O_3$	$Y_2O_3 + (12/7)Ti \rightarrow (3/7)Ti_4O_7 + 2Y$
$ZrO_2 + (6/5)Ti \rightarrow Zr + (2/5)Ti_3O_5$	$Y_2O_3 + (3/2)Ti \rightarrow (3/2)TiO_2 + 2Y$
$ZrO_2 + (8/7)Ti \rightarrow Zr + (2/7)Ti_4O_7$	$Y_2O_3 + 3Ti \rightarrow 3TiO + 2Y$
$ZrO_2 + 2Ni \rightarrow Zr + 2NiO$	$Y_2O_3 + 3Ni \rightarrow 3NiO + 2Y$
$(3/2)ZrO_2 + 2Al \rightarrow Al_2O_3 + (3/2)Zr$	$Y_2O_3 + 2Al \rightarrow Al_2O_3 + 2Y$
$ZrO_2 + Si \rightarrow SiO_2 + Zr$	$Y_2O_3 + (3/2)Si \rightarrow (3/2)SiO_2 + 2Y$

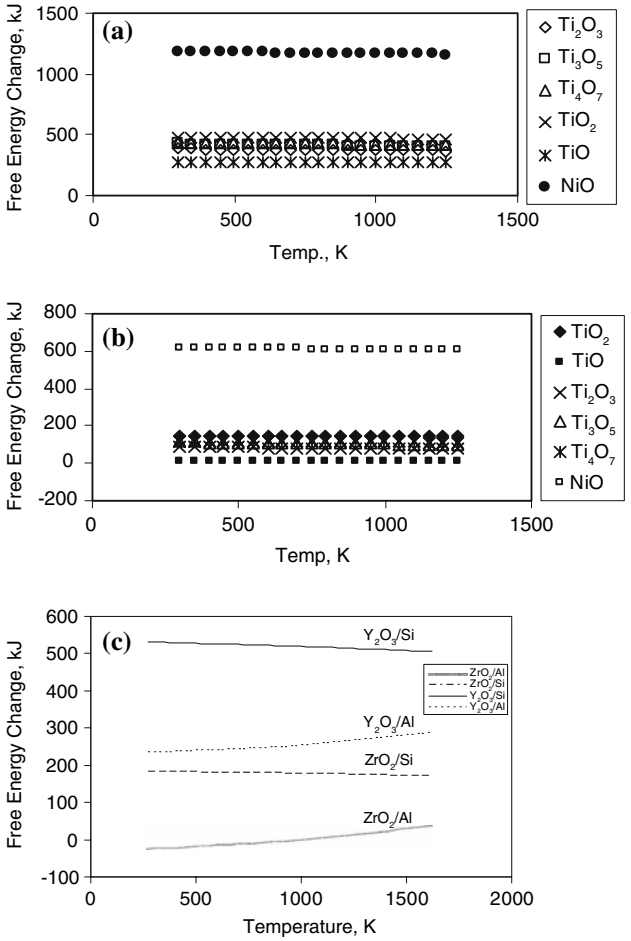

Fig. 9 Free energy of possible chemical reactions (listed in Table 5) between Ti and (**a**) zirconia and (**b**) yttria, and (**c**) between Al or Si and zirconia or yttria

Table 6 Wetting index of silver brazes on different grades of stainless steel [14]

Braze	*T*, K	Wetting index, WI	
		316 SS	304 SS
T50	1,123	0.024	–
	1,173	0.038	0.026
	1,223	0.062	0.057
	1,273	–	–
T51	1,073	0.007	–
	1,123	0.029	–
	1,173	0.039	–
	1,223	–	0.029
	1,273	–	0.082
T52	1,123	0.027	0.001
	1,173	0.045	0.014
	1,223	0.063	0.045
	1,273	–	0.09

Braze composition (in wt%): T50 (62.5Ag–32.5Cu–5Ni), T51 (75Ag–24.5Cu–0.5Ni), and T52 (77Ag–21Cu–2Ni)

Table 7 Contact angle (θ) and work of adhesion (W_{ad}) of zirconia ceramics with the steel and braze constituents [16–20]

System	*T*, K	θ, deg.	W_{ad}^{a}, J m^{-2}
ZrO_2/Cu	1,473	122.18[8]	0.602[8]
ZrO_2/Ag	1,373	73 ± 8[7], 121.7[9]	1.202[7],0.423[9]
ZrO_2/Ni	1,740	122.33	0.814
ZrO_2/Ni	1,773	118.1[4], 136.7[5], 120.3[6]	0.432[4], 0.222[5], 0.405[6]
ZrO_2/Fe	1,823	92[4], 111[5], 102[6]	1.832[4], 1.218[5], 1.504[6]
YSZ/Ni	1,773	117[1], 105[2]	0.446, 0.606
YSZ/Ni–2%Ti	1,773	129[1], 107[2], 30[3]	–
CSZ[9]/Ni	1,773	–	0.943

[a] W_{ad} is the work of adhesion. W_{ad} values are either from the cited work, or calculated using the σ_{lv} values at the designated temperatures using the temperature-coefficients of surface tension of liquid metals from [15]. [1] Mo susceptor in the heater, and Ar–4%H_2 atmosphere; [2] graphite susceptor, and Ar atmosphere; [3] graphite susceptor, and Ar–4%H_2 atmosphere; [4] in vacuum; [5] in H_2 atmosphere; [6] in He atmosphere; [7] in air; [8] in argon atmosphere, [9] CaO-stabilized zirconia

made by covering nearly the entire YSZ and steel surfaces with the same size braze foil; thus, nominal braze/substrate contact area was constant but the real contact was established essentially by the capillary penetration of surface roughness (troughs) which was facilitated by the presence of Ti.

Microhardness

Knoop microhardness profiles in the joint region are shown in Fig. 10. Within the steel substrates, a fairly consistent hardness value of 150–160 KHN is attained; hardness is only marginally lower within the braze region, but a marked rise in KHN is obtained upon entering the YSZ region, which leads to a rather sharp discontinuity in

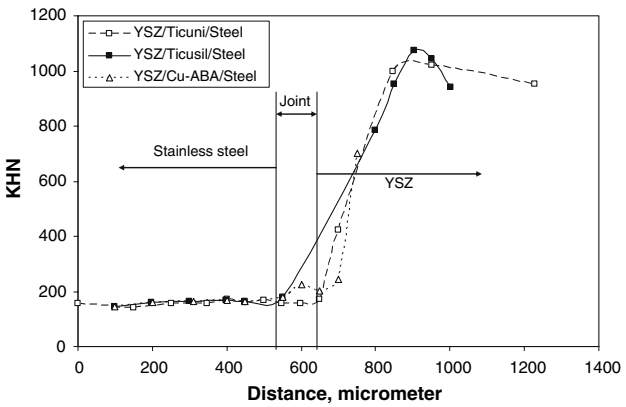

Fig. 10 Knoop microhardness across the YSZ/stainless steel joints made using Ticuni, Ticusil, and Cu-ABA braze foils

hardness profile at the YSZ/braze interface. Among the factors that influence the joint microhardness, thermal stresses due to the mismatch of coefficients of thermal expansion (α) play a major role. The CTE of steel (11×10^{-6}/K) is comparable to the CTE of YSZ (8.9 to 10.6×10^{-6}/K, average CTE $\sim 9.75 \times 10^{-6}$/K), but the CTE of the three brazes are rather high (CTE of Ticuni, Ticusil, and Cu-ABA are 20.3×10^{-6}/K, 18.5×10^{-6}/K, and 19.5×10^{-6}/K, respectively. These data indicate that tensile strains ($\Delta\alpha\Delta T$) may develop in the braze region due to differential contraction during cooling from the braze application temperature. These strains may, however, be accommodated via plastic flow resulting from the large ductility of the braze alloys (Table 1).

Conclusions

Three Cu-, Ag-, and Ti-base active filler metals (Cu-ABA, Ticuni, and Ticusil) were tested for high-temperature oxidation resistance to 750–850 °C, and for their effectiveness in joining yttria-stabilized-zirconia (YSZ) to a corrosion-resistant ferritic stainless steel for possible SOFC use. The oxidation kinetics of Ticusil are fastest, possibly due to the formation of unstable silver oxide (Ag_2O). The kinetics are slowest for the Cu-ABA, which showed marginal weight gain, and intermediate for Ticuni. Evidence of chemical interdiffusion between YSZ, steel, and braze led to compositional changes and interface reconstruction by reaction layer formation, which yielded metallurgically sound joints.

Acknowledgements The authors would like to thank Mr. John Setlock and Mark Jaster for their help at various stages of this work and Mr. Michael Halbig for critical review of the manuscript. R. Asthana acknowledges the research support received from the NASA Glenn Research Center.

References

1. Materials joining technology critical to future fuel cell manufacturing, EWI Insights (http://www.ewi.org), pp 4–5
2. Weil KS, Hardy JS Brazing a mixed ionic/electronic conductor to an oxidation-resistant metal. Adv Join Ceram, pp 185–198
3. Paiva OC, Ferreira L, Barbosa MA (1998) In: Bellosi A et al (eds) Interfacial science in ceramic joining. Kluwer Academic Publications, pp 329–340
4. Peteves SD, Ceccone G, Paulasto M, Stamos V, Yvon P (1996) JOM 48(1):48
5. Nichols MG, Peteves SD (1994) Reactive joining. Chemical effects on the formation and properties of brazed and diffusion-bonded interfaces. Scripta Mater 31(8):1091–1096
6. Nicholas MG (1988) In: Materials science forum, vol. 29. Trans Tech, Switzerland, pp 127–150
7. Hanson WB, Ironside KI, Fernie JA (2000) Acta Mater 48(18–19):4673
8. Hey AW (1990) In: Nicholas MG (eds) Joining of ceramics. Chapman & Hall, New York, p 66
9. Morizono Y, Nishida M, Chiba A, Nakata T (2004) J Ceramic Soc Japan 112(6):305
10. Loehman RE (1989) Ceramic Bull 68(4):891
11. Eustathopoulos N, Nicholas MG, Drevet B (1999) Wettability at high temperatures. Pergamon, p 348
12. Westbrook JH (ed) (1992) Moffatt's handbook of phase diagrams, vol. 2. Genium Publishing Co
13. Paulasto M, Ceccone G, Peteves SD (1997) In: Eustathopoulos N, Sobczak N (eds) High-temperature capillarity. Kracow, Poland
14. Metals Handbook, vol. 6, Welding, brazing and soldering. ASM International, Materials Park, OH, pp 117–118
15. Keene BJ (1993) Int Mater Revs 38(4):157
16. Nikolopoulos P, Sotiropoulou S (1987) J Mater Sci Lett 6:1429
17. Grigorenko NF, Stegny AI, Kasich-Pilipenko IE, Naidich YV, Pasichny VV (1994) In: Eustathopoulos N (ed) High-temperature capillarity. Slovak Acad Sci, Bratislava, p 123
18. Sotiropoulou D, Nikolopoulos P (1993) J Mater Sci 28:356
19. Humenik M Jr, Kingery WD (1954) J Am Ceramic Soc 37(1):18
20. Tsoga A, Naoumidis A, Nikolopoulos P (1996) Acta Mater 44(9):3679
21. Perevertailo VM, Loginova OB, Bagno NG (2001) In: Trans. Joining & Welding Res. Institute, JWRI, Osaka University, Japan, 30, pp 143–147
22. Kanetkar CS, Kacar AS, Stefanescu DM (1988) Metall Mater Trans 19A:1833